

1 Planar cell polarity: intracellular 2 asymmetry and supracellular 3 gradients of Dachous

4
5 Adrià Chorro¹, Bhavna Verma², Maylin Homfeldt³, Beatriz Ibáñez⁴, Peter A.
6 Lawrence✉ and José Casal✉

7 Department of Zoology, University of Cambridge, Downing Street, Cambridge CB2
8 3EJ, United Kingdom

9 Summary

10 **The slope of a supracellular molecular gradient has long been thought to**
11 **orient and coordinate planar cell polarity (PCP). Here we demonstrate and**
12 **measure that gradient. Dachous (Ds) is a conserved and elemental**
13 **molecule of PCP; Ds forms intercellular bridges with another cadherin**
14 **molecule, Fat (Ft), an interaction modulated by the Golgi protein Four-**
15 **jointed (Fj). Using genetic mosaics and tagged Ds we measure Ds *in vivo* in**
16 **membranes of individual cells over a whole metamere of the *Drosophila***
17 **abdomen. We find: 1. A supracellular gradient that rises from head to tail in**
18 **the anterior compartment (A) and then falls in the posterior compartment**
19 **(P). 2. There is more Ds in the front than the rear membranes of all cells in**
20 **the A compartment, except that compartment's most anterior and most**
21 **posterior cells. There is more Ds in the rear than in the front membranes of**
22 **all cells of the P compartment 3. The loss of Fj removes intracellular**
23 **asymmetry anteriorly in the segment and reduces it elsewhere. Additional**
24 **experiments show that Fj makes PCP more robust. Using Dachs (D) as a**
25 **molecular indicator of polarity, we confirm that opposing gradients of PCP**
26 **meet slightly out of register with compartment boundaries.**

27 Background

28 (i) A brief history of PCP

29 *“We have, then, to imagine a system where the polarity of the cells depends on,*
30 *or is, the direction of slope of a gradient” [1].*

31 *“It is assumed that a concentration gradient exists between the frontal and the*
32 *caudal margin of the segment. In Galleria the scales [...] orient in the direction of*
33 *the steepest gradient” [2].*

34 Animals are largely constructed from epithelia and information about polarity
35 within the epithelial plane is essential for organised development. For example,
36 appendages must be built in the correct orientation, cilia must beat together in
37 the right direction, vertebrate hairs and insect bristles must point accurately.
38 This process must be coordinated as fields of cells usually share the same
39 polarity. This property is referred to as planar cell polarity or PCP [3] and the
40 mechanisms responsible for it have been investigated by transplantation,
41 genetics, genetic mosaics, molecular biology and modelling.

42 The orientation of cells must relate to the developmental landscape; where
43 is the head? where is the midline? Does this necessary information rely on a
44 molecular device that, with reference to embryonic anatomy, points an arrow
45 rather as a magnetic field orients a compass needle? If so, we would need to
46 explain how polarity information is set up in relation to the main axes of the
47 body, how it is conveyed to the cells and how it is read locally. Long ago,
48 Lawrence [1] and Stumpf [2] proposed independently, on the basis of
49 experimental results in different insects, that the scalar values and slopes of
50 morphogen gradients could provide both positional information and orienting
51 information to the cells. A morphogen gradient was then imagined to be a
52 supracellular concentration gradient of secreted molecules that is aligned to the
53 axes of body or organ. The arrow of PCP would be a readout of the direction of
54 slope of that gradient.

55 When research into PCP began [1-5] the genes responsible were not known
56 but subsequently *Drosophila* genetics was applied to the problem, mutations that
57 interfered with cell polarisation were studied and several instrumental genes

58 identified [eg **6**, **7**]. Later, genes homologous to those in *Drosophila* were found in
59 vertebrates and elsewhere and shown to be engaged in PCP. A nice example of
60 this conservation is the stereocilia of the vertebrate inner ear whose exact
61 orientation is critical for balance and hearing; attempts to analyse this process
62 have been based on studies of PCP in the fruitfly [**8**].

63 After PCP genes were identified and sequenced many have worked to
64 understand what these proteins do. Genetic mosaics have proved to be a key
65 method. Let's take an early and important example: mutations in the *frizzled* (*fz*)
66 gene cause disturbance of PCP, but what happens if a small clone of cells that lack
67 the gene are surrounded by normal cells? Gubb and Garcia-Bellido [**9**] found that
68 although the *fz*⁻ clone itself produces disoriented hairs, several rows of the
69 genetically normal cells surrounding the mutant patch were reoriented to point
70 towards the clone, suggesting that cell interaction is a key element of the whole
71 process.

72 From many years of research, it has become apparent that PCP is not
73 directly but indirectly dependent on the slope of gradients of morphogens.
74 Epithelial cells are oriented by gradients of other (PCP) molecules whose
75 synthesis is regulated by and downstream of the morphogens themselves. Also,
76 experiments have evidenced that there are two independent molecular systems
77 of PCP; in both cell interaction is an important component and each system can
78 act alone to polarise cells. Both systems are independently oriented by
79 morphogen gradients [**10**]. These two systems may act in support or in
80 opposition to each other. Each of these systems depend on a specific set of
81 molecules that form bridges between adjacent cells [**10**, reviewed in **11**, **12**, **13**].

82 (ii) The Dachshous/Fat system

83 Here we study one of these two molecular systems, the Ds/Ft system. Mutations
84 affecting Ds and Ft cause misoriented cells. Their genes were found to specify
85 large atypical protocadherin molecules. A Ft molecule in one cell is thought to
86 bind to a Ds molecule in the other cell, thereby stabilising both molecules in the
87 cell membranes and forming a heterodimeric bridge from cell to cell [**14**, **15**].
88 Consequently, the accumulation of one molecule, say Ft, in a cell can affect the

89 disposition of the other molecule, Ds, in the neighbouring cell — whose polarity
90 may thus be altered, affecting the next neighbouring cell and so on [10].

91 The orientations of many cells are thought to be coordinated by one
92 supracellular gradient of Ds activity. The shape of this gradient may be
93 determined by not only the distribution of Ds protein itself but also, in the eye,
94 by an opposing supracellular gradient of Fj [16]. Fj is a Golgi-resident kinase
95 molecule that reduces the activity of Ds (in its binding to Ft) and increases the
96 activity of Ft (in its binding to Ds) [17, 18]. See [figure 1](#) for a summary.

97 Yang et al [19] made the first observations suggesting that, in the
98 *Drosophila* eye, Ds and Fj are distributed in opposing gradients whose
99 orientation relates to ommatidial polarity. Similarly, in the adult abdomen, Casal
100 et al [20] deduced from studying mutant clones and enhancer traps that,
101 normally, Ds is graded in opposite directions in the A and P compartments and
102 that Fj is also graded, but in the opposite sense to Ds, in both compartments.
103 Evidence from enhancer traps and genetic mosaics have argued that both Ds and
104 Fj are present in opposing gradients of function also in the eye and the wing [21,
105 22] but we have no precise picture of the ranges, the shapes or the steepness of
106 the gradients in any of these organs. There is an earlier molecular investigation
107 of Ds in the abdominal metamere which indicates that there are gradients of
108 amount [23]. We assess this data as supportive of gradients but preliminary—
109 their quantitation does not measure the amount of Ds on single membranes
110 (which we believe to be necessary) but records the distribution of Ds on joint
111 membranes. No quantified data is provided and therefore the slope of any
112 gradients remain unknown (Fig. 4 of their paper). Also, it was assumed that the
113 boundaries of gradients are colinear with the lineage boundaries, which as we
114 show below was not a correct assumption.

115 Evidence that the Ds/Ft system can drive PCP directly — and not via the
116 Stan/Fz system, as had been proposed [19, 24, reviewed in 25] — came from
117 experiments by Casal et al. [10] in the abdomen [reviewed in 26]. But that
118 finding raised the question: how does it do so? We proposed that the numbers of
119 bridges and their orientations (Ds-Ft or Ft-Ds) differed in amounts between the
120 anterior and posterior membranes of each polarised cell (numbers that together

121 determine the intracellular asymmetry). That molecular asymmetry within
122 single cells was measured by Strutt's group but only in a small area of the wing
123 disc near the peak of the gradient of Ds [27] and where the cells are strongly
124 asymmetric in the localisation of Dachs. Here we assess both the intracellular
125 asymmetry and the supracellular gradient by measuring the amount of Ds of all
126 single membranes over a whole metamere of the abdomen. We also study and
127 analyse the effect of Fj on these parameters and explain its role in the Ds/Ft
128 system itself. The abdomen was chosen as it is made up of atavistic segments
129 rather than the wing or the eye which are appendages. Finally, and this is an
130 important advantage, only in the abdomen is there a simple relationship
131 between the axis of PCP (the hairs and denticles point posteriorly) and the main
132 axis of the body (the anteroposterior axis).

133 Materials and Methods

134 Mutations and transgenes

135 Flies were reared at 25°C on standard food. The FlyBase [28] entries for the
136 mutant alleles and transgenes used in this work are the following:

137 *hs.FLP*: *Scer\FLP1^{hs.PS}*; *tub.Gal4*: *Scer\GAL4^{alphaTub84B}*; *UAS.nls-GFP*:
138 *Avic\GFP^{UAS.Tag:MYC,Tag:NLS(SV40-largeT)}*; *tub.Gal80*: *Scer\GAL80^{alphaTub84}*; *UAS.fz*:
139 *fz^{Scer\UAS.cSa}*; *ff⁻*: *ff^{d1}*; *ds::EGFP*: *Avic\GFP^{ds-EGFP}*; *CycE⁻*: *CycE^{KG00239}*; *y⁺*: *Dp(1;2)sc¹⁹*;
140 *w⁺*: *w^{+30c}*; *en.Gal4*: *Scer\GAL4^{en-e16E}*; *UAS.DsRed*: *Disc\RFP^{UAS.cKa}*; *hs.CD2*:
141 *Rnor\Cd2^{hs.PJ}*; *UAS.ft*: *ft^{UAS.cMa}*; *act>stop>d::EGFP*: *d^{FRT.Act5C.EGFP}*.

142 Experimental genotypes

143 ***UAS.fz* clones**: *y w hs.FLP tub.Gal4 UAS.nls-GFP / y w hs.FLP; FRT42D tub.Gal80/*
144 *FRT42D pwn; UAS.fz/ +*

145 ***UAS.fz* clones in *ff⁻***: *y w hs.FLP tub.Gal4 UAS.nls-GFP / y w hs.FLP; FRT42D*
146 *tub.Gal80 ff⁻/ FRT42D pwn ff⁻; UAS.fz/ TM2*

147 **Untagged *ds* clones**: *y w hs.FLP; ds::EGFP CycE⁻ FRT40A / y⁺ w⁺ FRT40A en.Gal4*
148 *UAS.DsRed; +/- TM2*

149 **Untagged *ds* clones in *ff⁻***: *y w hs.FLP; ds::EGFP CycE⁻ FRT40A ff⁻/ y⁺ w⁺ FRT40A*
150 *ff⁻ en.Gal4 UAS.DsRed*

151 **UAS.ft clones:** *y w hs.FLP/ w; FRT42D pwn / FRT42D tub.Gal80 hs.CD2; UAS.ft /*
152 *tub.Gal4*

153 **d::GFP clones:** *y w hs.FLP/ w; +/y⁺ w⁺ FRT40A en.Gal4 UAS.DsRed;*
154 *act>stop>d::EGFP/ +*

155 **d::GFP clones in ff⁻:** *y w hs.FLP/ w; ff⁻/y⁺ w⁺ FRT40A ff⁻ en.Gal4 UAS.DsRed;*
156 *act>stop>d::EGFP/ +*

157 Cuticle clones

158 To induce clones overexpressing *fz* or *ft*, pupae of the appropriate genotypes
159 were heat shocked, at 96-120 hours after egg deposition, at 37°C for 30 minutes
160 in a water bath. 2-3 days after eclosion, adult flies were selected and kept in
161 tubes containing 70% ethanol. Cuticles were dissected and mounted in Hoyers
162 medium. Images were taken on a Zeiss Axiophot microscope (Carl Zeiss Ltd,
163 Cambourne, UK) equipped with Nomarski optics using a 40x/0.90 Plan-Neofluar
164 lens, a Nikon D-300 camera (Nikon Uk Ltd., Surbiton, UK) connected to an iMac
165 computer, and Nikon Camera Control Pro 2. Stacks of images taken at different
166 focal planes were combined into a single image with Helicon Focus (HeliconSoft,
167 Kharkiv, Ukraine).

168 Quantification of polarisation strength

169 Overlapping images of adult cuticles containing overexpressing *fz* clones,
170 labelled with *pawn*, were stitched together using Adobe Photoshop with the
171 object of including the whole pigmented and haired area of the A compartment
172 in a single image that was saved as a TIFF file. The file was opened with the
173 ImageJ bundle Fiji. The segmented line tool was used to estimate the size of the A
174 compartment using pigmentation and hairs as landmarks [29], to measure the
175 average distance between the anterior boundary of the A compartment and the
176 anterior border of the clone, and the average length of the cuticle anterior to the
177 clone that showed reversed polarization. Due to the irregular shape of the clones
178 the measurements were done at three different positions for each clone and the
179 resultant average was used for the final plot. Note that for clones in the anterior
180 [a2 region 29] of the A compartment, measurement of effect was limited, not by
181 the extent of repolarisation but by the lack of hairs in the *a1* region. Therefore
182 clones close to the anterior boundary of hairs were not scored.

183 Live imaging of pupal epidermis

184 To induce clones expressing *ds::GFP* or untagged *ds* clones, pupae of the
185 appropriate genotypes were heat shocked at 24 hours after puparium formation
186 at 33°C for 5 or 15 minutes respectively in a water bath. 24 hours later, a 2x2 cm
187 spacer was prepared with 7 layers of double-sided tape (Tesafix 4964, Tesa UK
188 Ltd., Milton Keynes, UK), and a hole 6 mm in diameter was punched out of the
189 centre; the spacer was attached to a microscope slide. Each pupa was removed
190 from the puparium, transferred to the hole with its dorsal side facing up, covered
191 with Voltalef 10S oil (VWR International, Lutterworth, UK) and sealed with a
192 coverslip. Epidermal cells in the A3–A5 abdominal segments of the pupa were
193 imaged live using a Leica SP5 inverted confocal microscope with a 63×/1.4 oil
194 immersion objective. Tagged fluorescent proteins were excited sequentially with
195 488 nm and 561 nm laser beams and detected with 500 – 540 nm and 570 – 630
196 nm emission filters, using Leica HyD hybrid detectors. To maximise the dynamic
197 range and avoid clipping, the pixel depth was set to 12 bits and the gain and laser
198 power adjusted appropriately. Stacks of 1024 x1024 pixel images were thus
199 acquired.

200 Quantification of Ds

201 Image stacks were opened in Fiji, and projected into a single image with the
202 Maximun intensity projection algorithm. Background was subtracted with a
203 Rolling Ball of 6 pixels. The coordinates of the A/P and P/A boundaries
204 (determined by the limits of *engrailed* expression) were obtained, as well of the
205 average fluorescence intensity of the Ds signal in a 40x15 pixel box situated in a
206 region of the A compartment free of clones and abutting the A/P boundary. Using
207 the Freehand tool with a 6 pixel width, we measured the intensity of the Ds
208 signal at the posterior and anterior border of untagged Ds clones (i.e. the
209 intensity of the signal originated from a single anterior or posterior cell
210 membrane, see Figure 1), recording the average of the intensity of three separate
211 measures. Twin clones carrying two doses of *ds::EGFP* would be also
212 homozygous for a *Cyclin E* mutation rendering them unable to proliferate. The
213 coordinates of the centre of each freehand line was also obtained, allowing us to
214 determine the position of the clone borders relative to the length of the A or P

215 compartments. Each fluorescence intensity was standardized with respect to the
216 intensity of the box measured before, and finally the *Relative Levels* calculated as
217 $\log(\text{Relative Intensity}) - 3$.

218 **Statistics and Plotting**

219 We used RStudio with R v.4.1.2 [30], and the tidyverse, readxl, patchwork,
220 ggpubr, tidymodels, rstatix, and mgcv packages.

221 **Results**

222 There are several interrelated projects:

223 1. We measure the differences in Ds amounts on opposite sides of individual
224 diploid cells (histoblasts) across the whole abdominal metamere of the living
225 pupa. This same data tells us also how the amount of membraneous Ds varies
226 across an entire segment, each segment comprising one A and one P
227 compartment.

228 2. We study the contribution of Fj to the Ds/Ft system with respect to the
229 metameres.

230 3. We map the molecular polarity of every cell in a segment using Dachs.

231 Here we use a normally regulated and fluorescently tagged Ds molecule
232 [thanks to 27]. To measure the tagged Ds in any one cell membrane its protein
233 must be singled out from any fluorescent signal contributed by the abutting
234 membrane of a neighbour cell — this is achieved by making many patches
235 (clones) of cells that contain only untagged Ds, thereby isolating single
236 membranes bearing tagged Ds that face the periphery of these clones (see
237 Material and Methods).

238 **(i) Supracellular distribution of Ds across an abdominal metamere**

239 In a single metamere of the pupal abdomen about 37 cells were counted along
240 the anteroposterior axis from front to back of the A compartment and about 11
241 cells spanned the P compartment (all cell divisions having stopped by this stage).

242 To find the distribution of Ds, we sampled along the anteroposterior axis,
243 these numbers are then plotted against segment length. We report a
244 supracellular gradient in the A compartment in which Ds increases in amount

245 towards the rear as predicted [**10**, **20**, see also **23**]; a quasilinear correlation is
246 clearly seen and is robust and statistically significant (**figure 2a**). We find that the
247 Ds gradient rises steadily to achieve a difference in relative levels of 30%
248 between its posterior and anterior limits. This quantitation confirms that the
249 supracellular gradient of Ds in the P compartment is reversed to show a
250 difference in amount between its anterior and posterior limits of about 15%
251 (**figure 2a**).

252 (ii) Cellular asymmetry measured across an abdominal metamere.

253 The results are shown (**figure 2b**). The data for the anterior and posterior
254 membranes are plotted separately. As predicted [**10**], within the A compartment
255 the anterior membranes contain more Ds than the posterior with the relative
256 levels changing across the segment. In the P compartment there is cellular
257 asymmetry also but with the opposite sign (high in the posterior membrane, as
258 expected). In the P compartment this asymmetry is statistically secure only in
259 the central region located away from the A/P and P/A borders.

260 The maximum difference of relative levels of Ds between the anterior and
261 posterior membranes occurs in the middle of each compartment being ca 40% in
262 the A compartment and ca 20% in the P (**figure 2b**).

263 (iii) Cellular asymmetry and supracellular gradients in the absence of Fj

264 Fj is clearly part of the Ds/Ft system, but the loss of Fj causes only slight effects
265 on the wildtype phenotype. Nevertheless, comparing ff^+ and ff^- genotypes of the
266 A compartment we find that the cellular asymmetry is significantly reduced
267 relative to wildtype, most clearly in the anterior 20% of the A compartment
268 (compare **figures 2b and 3b**). A superposition of the data from both genotypes
269 shows that, remarkably, the accumulation of Ds in the anterior membranes is not
270 detectably affected by the removal of Fj (**figure 2c**). However, the relative levels
271 of Ds recorded on posterior membranes of the cells is decreased in ff^- as
272 compared to the wild type (**figure 2c**). The same comparison in the P
273 compartment (where, compared with the A compartment, the gradient and
274 cellular asymmetry are reversed) shows that the loss of Fj has its largest effect
275 also on the posterior membranes (**figure 2c**).

276 Note that the supracellular gradients of both wildtype and *ff*⁻ differ little
277 but there appears to be some reduction in the Ds gradient in *ff*⁻, again in the most
278 anterior region of the A compartment. (compare [figures 2b](#) and [3a](#)).

279 [\(iv\) Estimating the effects of Fj on the robustness of the Ds/Ft system.](#)

280 Even though the loss of Fj mainly affects the legs, the Fj protein may still have an
281 important function in the abdomen. It could be that Fj makes the Ds/Ft system
282 more robust and this is evidenced by a reduction in the asymmetric distribution
283 of Ds in the cellular membranes of *ff*⁻ cells (see above). This hypothesis can be
284 tested: we employ the Stan/Fz system to reverse polarity locally within the A
285 compartment and to succeed it must overcome the Ds/Ft system (which is trying
286 to maintain normal polarity). Thus, the more robust the Ds/Ft system is, the
287 better it will be able to resist and reduce the polarising effects of the Stan/Fz
288 system. We make small marked clones overexpressing *fz*, a key component of the
289 the Stan/Fz system; these cause all the cells around to point their hairs away
290 from the clones, an effect only readily apparent in those areas anterior to those
291 clones [31]. Comparing the polarity effects of *fz*-expressing clones in various
292 positions in the anteroposterior axis, one sees no clear trend in wildtype flies.
293 However, the local reversal of the polarity of bristles spreads much further in a
294 *ff*⁻ background, notably in the anterior region ([figure 4a](#)). These findings argue
295 that that Fj strengthens the robustness of the Ds/Ft system, particularly at the
296 front of the A compartment. This makes sense as there is indirect evidence that,
297 in the wildtype, the amount of Fj is graded within each segment, with the highest
298 amount anteriorly where *ff*⁻ clones show the strongest phenotype [20, 21].

299 [\(v\) Using Dachs to map cellular asymmetry throughout the pupal segment in](#)
300 [ff⁺ and ff⁻ flies.](#)

301 The plots of Ds distribution ([figure 2](#)) showed that the cellular asymmetries
302 dwindle and cross over near the A/P and P/A borders, not showing exactly
303 where the two opposing gradients meet and raising uncertainty as to where cell
304 polarity changes. Dachs (D) protein is an excellent indicator of the polarity of the
305 Ds/Ft system [32-34]. D is located on the membrane of the cell with the most Ds
306 and this polarity may or may not correlate with other indicators, such as the
307 pointing of adult hairs in the P compartment [23, 35]. Given that we find most of

308 the A compartment has a Ds gradient increasing posteriorly, are all the cells of
309 the A compartment polarised appropriately (according to current models, D
310 localises at the membrane where Ds is in excess [33], and therefore should be
311 localised anteriorly in the A compartment [10]). Given that most of the P
312 compartment has the opposite gradient, do all the cells of the P compartment
313 have D localised posteriorly? D localisation is reported to switch from anterior to
314 posterior polarity where the A and P compartments meet [23, 35]. However, we
315 re-examine this by means of the distribution of D in the pupal abdomen of both
316 wildtype and *ff*⁻ flies, using small clones carrying tagged D in a background in
317 which none of the D is tagged. In many cells it is obvious whether D accumulates
318 mainly or only on the anterior or posterior side. The results show that in the
319 wildtype, in **most** of the A compartment D is found in the anterior membrane
320 (figure 5a) and in **every cell** of the P compartment D is located in the posterior
321 membrane (figure 5b). Within the A compartment, about two rows of the most
322 anterior cells (figure 5c) and about two rows of the most posterior cells (figure
323 5d) show D located posteriorly, meaning that their Ds/Ft polarity is that
324 normally characteristic of the P cells. The larva, having fewer but larger
325 polyploid cells told a similar story: a set of cells in the A compartment, those
326 confined to the extreme posterior row, had variable polarity with some showing
327 the same polarity as in the P compartment [D accumulating posteriorly 36].

328 These findings place alternating fields of polarity out of register with the
329 corresponding compartments and raise questions about the role of the
330 compartment boundary in the genesis of polarity [cf 20]. We therefore decided
331 to make polarity-changing clones that overexpress *ft* in order to alter polarity
332 near compartment boundaries. Normally such *ft*-expressing clones will reverse
333 the polarity of surrounding cells depending on the compartment (hairs point
334 away from the clone in the A compartment and towards it in the P). One might
335 expect a *ft*-expressing clone located posteriorly in the A compartment and
336 touching the compartment boundary to behave like a normal A clone at the front
337 and reverse the polarity of wildtype cells in front of the clone, and it does so (the
338 wildtype hairs anterior to the clone now pointing away from the clone; see figure
339 6a). One would expect that such a clone would meet P cells at its posterior edge
340 and reverse the hairs behind the clone, and it does so (the wildtype hairs

341 posterior to the clone now pointing towards the clone; see [figure 6a](#)).
342 Correspondingly, one would expect that a clone located at the front of the P
343 compartment and contacting the A/P boundary to reverse both at front and
344 behind, but it fails to reverse hairs in front ([figure 6b](#)). The explanation for both
345 types of clones is simple: because the line of polarity reversal lies anterior to the
346 lineage boundary, an A clone contacts A cells in front of it and P cells behind.
347 However, the anterior extension of a P clone will be stopped at the A/P boundary
348 and cannot reach the line of polarity reversal (thus it contacts cells behaving as P
349 cells in front and therefore cannot reverse their polarity; see [figure 6c](#)).

350 In the flies lacking Fj, unlike in the wildtype, many cells in the anterior
351 region of the segment show reduced polarity, with D being distributed evenly
352 around the cell membrane. We think this finding correlates with our observation
353 (above) that the most anterior region of the segment is where the robustness of
354 the Ds/Ft system is most dependent on Fj. It is also pertinent that cells in the
355 anterior region of the segment show loss of Ds asymmetry when Fj is removed
356 ([figure 3b](#)). It also fits with the slight abdominal phenotype observed in *ff*⁻ flies,
357 in which there was some loss of normal polarity but only in the anterior region of
358 the segment [20, 21]. Thus, all these findings point to the same conclusion: in
359 cells of the anterior region of the segment, the polarisation by the Ds/Ft system
360 depends more on a gradient of Fj and less on a gradient of Ds — while in the
361 middle and rear of the A compartment the opposite is the case.

362 Discussion

363 Here we take the familiar model system of the *Drosophila* abdomen, in this case
364 at the pupal stage, and measure the distribution of Dachshous (Ds) in the
365 membranes of cells *in vivo*. We describe the intercellular gradients and
366 intracellular asymmetry across a whole metamere. Ds is distributed in a gradient
367 which is reflexed, rising in one direction in the A compartment of each metamere
368 and falling in the P compartment ([figure 2a](#)). Although this pattern resembles
369 that of a morphogen, our view is that Ds/Ft is not a morphogen: the primary
370 function of a morphogen is to provide positional information to the cells in its
371 field [reviewed in 37, 38], while the immediate purpose of the Ds/Ft gradient is
372 to polarise cells. Also, and unlike an archetypal morphogen, Ds does not move

373 from cell to cell, although the numbers of Ds molecules in the membrane of one
374 cell affect the distribution of Ft and Ds molecules in the adjacent cell [10]. There
375 are models of how the Ds/Ft system works, how polarity information passes
376 from cell to cell and how a gradient of Ds activity might point the arrow of
377 polarity [10, 13, 39, 40]. Our results validate the hypothesis that the orientation
378 of molecular gradients determines the polarity of the cells [1, 2].

379 The amount of Ds forms a linear gradient along the anteroposterior axis of
380 the A compartment, rising about 30%. We measure the cellular asymmetry in the
381 distribution of Ds across the whole metamere. In the A compartment it is
382 uniform and higher in the anterior membrane of the cell, that facing the bottom
383 of the gradient, that in the posterior membrane, that facing the top of the
384 gradient [as predicted 10]. In the P compartment both the direction of slope of
385 the gradient and its asymmetrical distribution in the cell are opposite to that in
386 the A compartment [10]. The difference between anterior and posterior
387 membranes is far less to that found when a small region of the wing imaginal
388 disk was studied [twofold 27]. However, modelling predicted that the difference
389 in the primordium of the wing disc could be less than twofold [39].

390 [The function of Fj](#)

391 There is considerable evidence from enhancer traps and from functional
392 experiments that Fj forms a gradient [16, 20, 21]. In the A compartment of each
393 abdominal segment it is evidenced to be highest in the most anterior region [20].
394 Fj phosphorylates both Ds and Ft proteins [41], the effect on Ds is to decrease its
395 affinity for Ft, while phosphorylated Ft has an increased affinity for Ds [17, 18].
396 It is thought that the two opposing gradients, Ds and Fj, work together to
397 produce asymmetric distributions of Ds-Ft bridges [10, 18]. Most pertinently,
398 Hale et al [39] have used FRAP to investigate the stability of Ds-Ft heterodimers
399 in the wing disk and observed differences between *ff*⁺ and *ff*⁻ flies. They
400 concluded that “the overall result of removing Fj was a reduction in stability of
401 the Ft-Ds dimer”. We cannot divine from this how the stability of bridges might
402 impact on cell asymmetry in different parts of the abdominal segment. This is
403 partly because Hale et al look at the conjoined membranes of two cells while we
404 distinguish anterior from posterior membranes of each cell. We do find that

405 removing Fj increases the relative amount of Ds in the posterior membrane over
406 much of the A compartment. Since Ds is stable in the membrane only when
407 joined to Ft in the next cell [14] it follows there should be more bridges in *ff*-
408 segments, and, if so, how can these bridges be less stable? Hale et al [39] also
409 deduced that the action of Fj on Ft dominated over its effect on Ds; however this
410 finding applied to their sample area (the wing pouch) which is near the top of the
411 Fj gradient; they do not tell us what, if any, might be the function of Fj in areas
412 where Ds expression is high but Fj low. Our data concern the whole field and
413 argue that Fj is essential for cellular asymmetry in only the anterior part of the A
414 compartment (where it peaks in the wildtype), but it is also needed in the rest of
415 the compartment to achieve a robust cellular asymmetry.

416 Perhaps the most problematic fact about Fj is that removing it has little
417 overt effect on phenotype. Nevertheless, in *ff*- flies, we found changes in Ds
418 distribution and a loss of robustness —shown by a reduction of the Ds/Ft
419 system's ability to resist polarity changes induced by clones in the Stan/Fz
420 system. Strikingly, in the anterior ca 20% of the A compartment, the loss of Fj
421 tends to totally depolarise the cells, eliminating the asymmetric distribution of
422 Ds, and reducing the asymmetric localisation of D. We conclude that the main
423 function of Fj in the abdomen, via its action on Ds and Ft, is to strengthen the
424 Ds/Ft system mainly at the front of the A compartment where Ft is high and Ds is
425 low.

426 Another clear finding demands an explanation: when the localisations of Ds
427 in *ff*⁺ and *ff*- flies are compared, they differ considerably, but only in the posterior
428 membranes of the cells (figure 3). It seems that Fj promotes the presence of Ds-
429 Ft dimers more strongly in the posterior than in the anterior membranes. We
430 offer a speculative model to explain this (figure 7).

431 The ranges of the Ds gradients

432 In order to map the polarity of all the cells individually we looked at tagged D,
433 whose asymmetric distribution depends on the localisation of Ds and Ft in the
434 cell [32, 33]. We expected [20] and it was even reported by others [23, 35] that
435 this inflection of cell polarity as well as the limits of the Ds/Ft gradients would
436 coincide at the A/P borders. However, our maps of D asymmetry make clear that

437 the changeover of polarity occurs not at the compartment border but just within
438 the A compartment —a result that at last makes sense of earlier findings with
439 clones overexpressing *ff*. Generally in the A compartment, hairs pointed away
440 from the clones (suggesting a Ds gradient that rose from anterior to posterior)
441 and, in the P compartment, hairs pointed towards the clones (suggesting a Ds
442 gradient that rose from posterior to anterior) [20]. However, the behaviour of
443 some *ff*-expressing clones, those that contacted a compartment border, did not fit
444 with our expectation at that time. For example, clones belonging to the P
445 compartment that reached the very front edge of the P compartment should
446 reverse the polarity of A cells in front but did not do so. Why not? We were
447 flummoxed and offered an *ad hoc* explanation [20]. Now we know that cells at
448 the extreme rear of the A compartment have the Ds/Ft polarity of P cells, a
449 simpler explanation makes more sense. Because *ft* and *ff*-expressing clones in the
450 P compartment are not able to extend across the compartment boundary to
451 contact cells with normal A polarity, they must, as observed, continue to behave
452 as a P clones at their anterior margins because, although they confront cells of A
453 lineage, those cells have the polarity of P cells. Consequently, effects on the
454 disposition of bridges will reinforce, rather than alter, normal polarity.

455 This new picture recalls other effects of compartmental borders in fly
456 development. An example is the A/P wing border. The interface between a
457 signalling P and a receiving A compartment leads to a signal (Hedgehog) crossing
458 over from P to A and initiating a response in the first cells of the receiving
459 compartment (turning on Dpp expression, [42, 43]. We wonder if our finding
460 relates to this: could a signal coming from the P compartment during early
461 development initiate changes in the first cell row or two of the A compartment
462 that spread forwards and backwards from there to induce a reflexed Ds/Ft
463 gradient in the A and the P compartment? It is relevant that [44] have argued
464 that the Ds/Ft gradient might be initially aligned in the anteroposterior axis in
465 the pupal wing (that is, orthogonal to hair orientation). In which case a Ds/Ft
466 gradient in the wing could also relate to a signal, such as Hedgehog, crossing over
467 the boundary from the P compartment into A.

468 Steepness model and growth

469 In thinking about the control of growth, and many have done so, we should
470 remember that it is likely to be complicated and multifactorial. For example,
471 regarding the role of the Ds/Ft system, removal of either Ft or Ds breaks that
472 system and yet the flies still grow. It follows that models relating to the Ds/Ft
473 system such as the steepness hypothesis [45, 46], or the feedforward model of
474 growth [47] may prove insufficient. Here we find that, within each compartment,
475 the difference between anterior and posterior membranes is largely uniform and
476 the supracellular gradient is largely linear. These are both prerequisites for the
477 simplest steepness model. In order to draw the arrow of PCP, anterior and
478 posterior membranes of a cell must be locally compared and for this there is
479 indirect evidence [48]. We conjectured that, in addition, the degree of difference
480 between these two cell membranes might feed into the decision as to whether a
481 cell divides or dies [45] and help to limit growth. This would amount to a
482 dimension-sensing mechanism. The steepness model is also supported by
483 experiments showing that interfaces between cells with different amounts of Ds
484 lead to Hippo target genes being activated and increased local growth across that
485 interface [49].

486 One or two systems?

487 We have argued that the Ds/Ft and Stan/Fz systems act independently [10, 26]
488 but this is not accepted by everyone [50]. Some authors have taken refuge in the
489 postulate that PCP might operate differently in various organs, so the two
490 systems might be independent in one organ (the abdomen) but are united in a
491 single pathway of function in other organs (eg, the wing) or that any direct action
492 of Ds/Ft on cell polarisation might constitute a “bypass pathway”. [22, 50]. We
493 view that refuge as intrinsically precarious. The many experiments and
494 contrasting interpretations in this area are well presented by Strutt and Strutt
495 [51]. The recent intervention of the Pk gene into this melée has not simplified
496 that debate [35, 52-55]. However, our results above (those comparing *fz*-
497 expressing clones in abdomens with and without Fj, figure 4, where we ask one
498 PCP system to act against the other), are simply explained if the systems act
499 independently. Under the alternative model, in which the Stan/Fz system is

500 presumed to act downstream of the Ds/Ft system, explaining the differing effects
501 of *fz*-expressing clones on polarity in *ff*⁺ and *ff*⁻ flies would tax the finest minds.
502 Our opinion is that the two systems can function distinctly everywhere and act in
503 conflict or in synergy. They interact late in the cellular process such as when
504 hairs are being formed in their final orientations.

505 [Some remaining questions](#)

506 There are many outstanding questions about the Ds/Ft system. Does the amount
507 of Ft vary over the field? What other factors, apart from Fj, modulate the
508 interaction of Ds and Ft molecules? How exactly is the supracellular gradient
509 read in order to orient polarity of cells? How are opposing membranes of a cell
510 compared in order to polarise that cell? Ds and Ft proteins are together localised
511 into puncta [56] but why are they and are puncta required for proper function?
512 We found the Ds/Ft gradient to be reflexed; consequently, since all the hairs
513 point posteriorly, they must be pointing up the Ds gradient in nearly all of the A
514 compartment and down the Ds gradient in the P compartment. How is this
515 achieved? One simple hypothesis is that hair polarity is the outcome, in the A
516 compartment, of both the Ds/Ft and the Stan/Fz systems instructing the hairs to
517 point posteriorly. However, in the P compartment, the Ds/Ft system aims to
518 point the hairs forward and the Stan/Fz aims to point backwards and, to put this
519 too simply, the Stan/Fz system wins. The *prickle* gene also plays a part in this, see
520 elsewhere [35, 51-54, 57].

521 [Data Accessibility](#)

522 Data used in figures ... and
523 <https://royalsocietypublishing.org/doi/10.1098/rsob.200290> -
524 [RSOB200290F8](#)..., electronic supplementary material, figures S... can be obtained
525 from the University of Cambridge Open Access repository
526 (<https://doi.org/10.17863/>...).

527 [Authors' Contributions](#)

528 The experiments were conceived of by JC and PAL, all the methods devised by JC.
529 Execution of the experiments including the making of genetic stocks depended

530 on all the authors. The paper was written by JC and PAL. All the authors gave
531 final approval for publication and agreed to be held accountable for their
532 contributions.

533 Conflict of Interest Declaration

534 Authors declare that they have no competing interests.

535 Funding

536 Our work was supported by Wellcome Investigator Award 107060 to P.A.L.

537 Acknowledgements

538 We thank David Strutt for his help and advice, Malcolm Burrows and Gary Struhl
539 for encouragement and the Wellcome Trust (4 grants), the Zoology Department
540 and the Newton Trust for supporting our experiments over the last 16 years.

541 Footnotes

542 †These two authors contributed equally to this work

543 ¹Present address: Institut Jacques Monod, UMR 7592, Université Paris Cité /
544 CNRS, Bâtiment Buffon, 15 rue Hélène Brion, 5205 Paris CEDEX 13, France

545 ²Present address: Department of Physiology, Anatomy and Genetics, Le Gros
546 Clark Building, South Parks Road, University of Oxford, Oxford OX1 3QX, United
547 Kingdom

548 ³Present address: Hochschule Bremen, Biomimetics-Innovation-Centre,
549 Neustadtswall 30, 28199, Bremen, Germany

550 ⁴Present address: UICEC, Centro de Documentación Clínica Avanzada, Hospital
551 Universitario Virgen del Rocío, Avd. Manuel Siurot s/n, 41013 Sevilla, Spain

552 Electronic supplementary material is available online at <https://doi.org/.../...>

553 References

554 1 Lawrence, P. A. 1966 Gradients in the insect segment: the orientation of
555 hairs in the milkweed bug *Oncopeltus fasciatus*. *J. Exp. Biol.* **44**, 607-620.
556 (10.1242/jeb.44.3.607)

- 557 2 Stumpf, H. F. 1966 Über gefälleabhängige Bildungen des
558 Insektensegmentes. *J. Insect Physiol.* **12**, 601-617. (10.1016/0022-
559 1910(66)90098-9)
- 560 3 Nübler-Jung, K. 1979 Pattern stability in the insect segment : II. The
561 intersegmental region. *Wilhelm Roux Arch. Dev. Biol.* **186**, 211-233.
562 (10.1007/BF00848590)
- 563 4 Wigglesworth, V. B. 1940 Local and general factors in the development of
564 "pattern" in *Rhodnius prolixus* (Hemiptera). *J. Exp. Biol.* **17**, 180-201.
- 565 5 Piepho, H. 1955 Über die polare Orientierung der Bälge und Schuppen auf
566 dem Schmetterlingsrumpf. *Biol. Zbl.* **74**, 467-474.
- 567 6 Adler, P. N. 1992 The genetic control of tissue polarity in *Drosophila*.
568 *Bioessays.* **14**, 735-741. (10.1002/bies.950141103)
- 569 7 Usui, T., Shima, Y., Shimada, Y., Hirano, S., Burgess, R. W., Schwarz, T. L.,
570 Takeichi, M., Uemura, T. 1999 Flamingo, a seven-pass transmembrane
571 cadherin, regulates planar cell polarity under the control of Frizzled. *Cell.*
572 **98**, 585-595. (10.1016/s0092-8674(00)80046-x)
- 573 8 Jones, C., Chen, P. 2007 Planar cell polarity signaling in vertebrates.
574 *Bioessays.* **29**, 120-132. (10.1002/bies.20526)
- 575 9 Gubb, D., Garcia-Bellido, A. 1982 A genetic analysis of the determination of
576 cuticular polarity during development in *Drosophila melanogaster*. *J.*
577 *Embryol. Exp. Morphol.* **68**, 37-57.
- 578 10 Casal, J., Lawrence, P. A., Struhl, G. 2006 Two separate molecular systems,
579 Dachous/Fat and Starry night/Frizzled, act independently to confer planar
580 cell polarity. *Development.* **133**, 4561-4572. (10.1242/dev.02641)
- 581 11 Carvajal-González, J. M., Mlodzik, M. 2014 Mechanisms of planar cell
582 polarity establishment in *Drosophila*. *F1000Prime Rep.* **6**, 98.
583 (10.12703/p6-98)
- 584 12 Goodrich, L. V., Strutt, D. 2011 Principles of planar polarity in animal
585 development. *Development.* **138**, 1877-1892. (10.1242/dev.054080)
- 586 13 Lawrence, P. A., Casal, J. 2018 Planar cell polarity: two genetic systems use
587 one mechanism to read gradients. *Development.* **145**, dev168229.
588 (10.1242/dev.168229)

- 589 14 Ma, D., Yang, C. H., McNeill, H., Simon, M. A., Axelrod, J. D. 2003 Fidelity in
590 planar cell polarity signalling. *Nature*. **421**, 543-547.
591 (10.1038/nature01366)
- 592 15 Matakatsu, H., Blair, S. S. 2004 Interactions between Fat and Dachsoous and
593 the regulation of planar cell polarity in the *Drosophila* wing. *Development*.
594 **131**, 3785-3794. (10.1242/dev.01254)
- 595 16 Zeidler, M. P., Perrimon, N., Strutt, D. I. 1999 The four-jointed gene is
596 required in the *Drosophila* eye for ommatidial polarity specification. *Curr.*
597 *Biol.* **9**, 1363-1372. (10.1016/s0960-9822(00)80081-0)
- 598 17 Brittle, A., Repiso, A., Casal, J., Lawrence, P. A., Strutt, D. 2010 Four-jointed
599 modulates growth and planar polarity by reducing the affinity of Dachsoous
600 for Fat. *Curr. Biol.* **20**, 803-810. (10.1016/j.cub.2010.03.056)
- 601 18 Simon, M. A., Xu, A., Ishikawa, H. O., Irvine, K. D. 2010 Modulation of
602 Fat:dDchsoous binding by the cadherin domain kinase Four-jointed. *Curr.*
603 *Biol.* **20**, 811-817. (10.1016/j.cub.2010.04.016)
- 604 19 Yang, C. H., Axelrod, J. D., Simon, M. A. 2002 Regulation of Frizzled by fat-
605 like cadherins during planar polarity signaling in the *Drosophila* compound
606 eye. *Cell*. **108**, 675-688. (10.1016/s0092-8674(02)00658-x)
- 607 20 Casal, J., Struhl, G., Lawrence, P. A. 2002 Developmental compartments and
608 planar polarity in *Drosophila*. *Curr. Biol.* **12**, 1189-1198. (10.1016/s0960-
609 9822(02)00974-0)
- 610 21 Zeidler, M. P., Perrimon, N., Strutt, D. I. 2000 Multiple roles for four-jointed
611 in planar polarity and limb patterning. *Dev. Biol.* **228**, 181-196.
612 (10.1006/dbio.2000.9940)
- 613 22 Simon, M. A. 2004 Planar cell polarity in the *Drosophila* eye is directed by
614 graded Four-jointed and Dachsoous expression. *Development*. **131**, 6175-
615 6184. (10.1242/dev.01550)
- 616 23 Mangione, F., Martin-Blanco, E. 2018 The Dachsoous/Fat/Four-jointed
617 pathway directs the uniform axial orientation of epithelial cells in the
618 *Drosophila* abdomen. *Cell Rep.* **25**, 2836-2850.
619 (10.1016/j.celrep.2018.11.036)
- 620 24 Adler, P. N., Charlton, J., Liu, J. 1998 Mutations in the cadherin superfamily
621 member gene dachsoous cause a tissue polarity phenotype by altering

- 622 frizzled signaling. *Development (Cambridge, England)*. **125**, 959-968.
623 (10.1242/dev.125.5.959)
- 624 25 Tree, D. R., Ma, D., Axelrod, J. D. 2002 A three-tiered mechanism for
625 regulation of planar cell polarity. *Semin. Cell Dev. Biol.* **13**, 217-224.
626 (10.1016/s1084-9521(02)00042-3)
- 627 26 Lawrence, P. A., Struhl, G., Casal, J. 2007 Planar cell polarity: one or two
628 pathways? *Nature Reviews. Genetics*. **8**, 555-563. (10.1038/nrg2125)
- 629 27 Brittle, A., Thomas, C., Strutt, D. 2012 Planar polarity specification through
630 asymmetric subcellular localization of Fat and Dachshous. *Curr. Biol.* **22**,
631 907-914. (10.1016/j.cub.2012.03.053)
- 632 28 Gramates, L. S., Agapite, J., Attrill, H., Calvi, B. R., Crosby, M. A., dos Santos,
633 G., Goodman, J. L., Goutte-Gattat, D., Jenkins, V. K., Kaufman, T., *et al.* 2022
634 FlyBase: a guided tour of highlighted features. *Genetics*. **220**,
635 (10.1093/genetics/iyac035)
- 636 29 Struhl, G., Barbash, D. A., Lawrence, P. A. 1997 Hedgehog organises the
637 pattern and polarity of epidermal cells in the *Drosophila* abdomen.
638 *Development*. **124**, 2143-2154.
- 639 30 R Core Team. R: A Language and Environment for Statistical Computing.
640 Vienna, Austria: R Foundation for Statistical Computing 2021.
- 641 31 Lawrence, P. A., Casal, J., Struhl, G. 2002 Towards a model of the
642 organisation of planar polarity and pattern in the *Drosophila* abdomen.
643 *Development*. **129**, 2749-2760.
- 644 32 Bosveld, F., Bonnet, I., Guirao, B., Tlili, S., Wang, Z., Petitalot, A., Marchand,
645 R., Bardet, P. L., Marcq, P., Graner, F., *et al.* 2012 Mechanical control of
646 morphogenesis by Fat/Dachshous/Four-jointed planar cell polarity
647 pathway. *Science*. **336**, 724-727. (10.1126/science.1221071)
- 648 33 Mao, Y., Rauskolb, C., Cho, E., Hu, W. L., Hayter, H., Minihan, G., Katz, F. N.,
649 Irvine, K. D. 2006 Dach: an unconventional myosin that functions
650 downstream of Fat to regulate growth, affinity and gene expression in
651 *Drosophila*. *Development*. **133**, 2539-2551. (10.1242/dev.02427)
- 652 34 Rogulja, D., Rauskolb, C., Irvine, K. D. 2008 Morphogen control of wing
653 growth through the Fat signaling pathway. *Dev. Cell*. **15**, 309-321.
654 (10.1016/j.devcel.2008.06.003)

- 655 35 Ambegaonkar, A. A., Irvine, K. D. 2015 Coordination of planar cell polarity
656 pathways through Spiny-legs. *eLife*. **4**, e09946. (10.7554/eLife.09946)
- 657 36 Pietra, S., Ng, K., Lawrence, P. A., Casal, J. 2020 Planar cell polarity in the
658 larval epidermis of *Drosophila* and the role of microtubules. *Open Biol.* **10**,
659 200290. (10.1098/rsob.200290)
- 660 37 Christian, J. L. 2012 Morphogen gradients in development: from form to
661 function. *Wiley Interdiscip. Rev. Dev. Biol.* **1**, 3-15. (10.1002/wdev.2)
- 662 38 Lawrence, P. A. 2001 Morphogens: how big is the big picture? *Nat. Cell Biol.*
663 **3**, E151-154. (10.1038/35083096)
- 664 39 Hale, R., Brittle, A. L., Fisher, K. H., Monk, N. A., Strutt, D. 2015 Cellular
665 interpretation of the long-range gradient of Four-jointed activity in the
666 *Drosophila* wing. *eLife*. **4**, e05789. (10.7554/eLife.05789)
- 667 40 Schamberg, S., Houston, P., Monk, N. A. M., Owen, M. R. 2010 Modelling and
668 Analysis of Planar Cell Polarity. *Bull. Math. Biol.* **72**, 645-680.
669 (10.1007/s11538-009-9464-0)
- 670 41 Ishikawa, H. O., Takeuchi, H., Haltiwanger, R. S., Irvine, K. D. 2008 Four-
671 jointed is a Golgi kinase that phosphorylates a subset of cadherin domains.
672 *Science*. **321**, 401-404. (10.1126/science.1158159)
- 673 42 Basler, K., Struhl, G. 1994 Compartment boundaries and the control of
674 *Drosophila* limb pattern by hedgehog protein. *Nature*. **368**, 208-214.
675 (10.1038/368208a0)
- 676 43 Lawrence, P. A., Struhl, G. 1996 Morphogens, compartments, and pattern:
677 lessons from *Drosophila*? *Cell*. **85**, 951-961. (10.1016/s0092-
678 8674(00)81297-0)
- 679 44 Merkel, M., Sagner, A., Gruber, F. S., Etoornay, R., Blasse, C., Myers, E., Eaton,
680 S., Julicher, F. 2014 The balance of prickle/spiny-legs isoforms controls the
681 amount of coupling between core and fat PCP systems. *Curr. Biol.* **24**, 2111-
682 2123. (10.1016/j.cub.2014.08.005)
- 683 45 Lawrence, P. A., Struhl, G., Casal, J. 2008 Do the protocadherins Fat and
684 Dachshous link up to determine both planar cell polarity and the dimensions
685 of organs? *Nat. Cell Biol.* **10**, 1379-1382. (10.1038/ncb1208-1379)
- 686 46 Bando, T., Mito, T., Maeda, Y., Nakamura, T., Ito, F., Watanabe, T., Ohuchi, H.,
687 Noji, S. 2009 Regulation of leg size and shape by the Dachshous/Fat

- 688 signalling pathway during regeneration. *Development*. **136**, 2235-2245.
689 (10.1242/dev.035204)
- 690 47 Zecca, M., Struhl, G. 2010 A feed-forward circuit linking wingless, fat-
691 dachsous signaling, and the warts-hippo pathway to *Drosophila* wing
692 growth. *PLoS Biol.* **8**, e1000386. (10.1371/journal.pbio.1000386)
- 693 48 Rovira, M., Saavedra, P., Casal, J., Lawrence, P. A. 2015 Regions within a
694 single epidermal cell of *Drosophila* can be planar polarised independently.
695 *eLife*. **4**, e06303. (10.7554/eLife.06303)
- 696 49 Willecke, M., Hamaratoglu, F., Sansores-Garcia, L., Tao, C., Halder, G. 2008
697 Boundaries of Dachous Cadherin activity modulate the Hippo signaling
698 pathway to induce cell proliferation. *Proc. Natl. Acad. Sci. U. S. A.* **105**,
699 14897-14902. (10.1073/pnas.0805201105)
- 700 50 Matis, M., Axelrod, J. D. 2013 Regulation of PCP by the Fat signaling
701 pathway. *Genes Dev.* **27**, 2207-2220. (10.1101/gad.228098.113)
- 702 51 Strutt, H., Strutt, D. 2021 How do the Fat-Dachsous and core planar polarity
703 pathways act together and independently to coordinate polarized cell
704 behaviours? *Open Biol.* **11**, 200356. (10.1098/rsob.200356)
- 705 52 Ayukawa, T., Akiyama, M., Mummery-Widmer, J. L., Stoeger, T., Sasaki, J.,
706 Knoblich, J. A., Senoo, H., Sasaki, T., Yamazaki, M. 2014 Dachous-dependent
707 asymmetric localization of spiny-legs determines planar cell polarity
708 orientation in *Drosophila*. *Cell Rep.* **8**, 610-621.
709 (10.1016/j.celrep.2014.06.009)
- 710 53 Olofsson, J., Sharp, K. A., Matis, M., Cho, B., Axelrod, J. D. 2014 Prickle/spiny-
711 legs isoforms control the polarity of the apical microtubule network in
712 planar cell polarity. *Development*. **141**, 2866-2874. (10.1242/dev.105932)
- 713 54 Sharp, K. A., Axelrod, J. D. 2016 Prickle isoforms control the direction of
714 tissue polarity by microtubule independent and dependent mechanisms.
715 *Biology Open*. **5**, 229-236. (10.1242/bio.016162)
- 716 55 Casal, J., Ibáñez-Jiménez, B., Lawrence, P. A. 2018 Planar cell polarity: the
717 *prickle* gene acts independently on both the Ds/Ft and the Stan/Fz systems.
718 *Development*. **145**, dev168112. (10.1242/dev.168112)
- 719 56 Strutt, H., Warrington, S. J., Strutt, D. 2011 Dynamics of core planar polarity
720 protein turnover and stable assembly into discrete membrane subdomains.
721 *Dev. Cell*. **20**, 511-525. (10.1016/j.devcel.2011.03.018)

- 722 57 Lawrence, P. A., Casal, J., Struhl, G. 2004 Cell interactions and planar
723 polarity in the abdominal epidermis of *Drosophila*. *Development*. **131**, 4651-
724 4664. (10.1242/dev.01351)
- 725 58 Allen, M., Poggiali, D., Whitaker, K., Marshall, T., van Langen, J., Kievit, R.
726 2021 Raincloud plots: a multi-platform tool for robust data visualization
727 [version 2; peer review: 2 approved]. *Wellcome Open Research*. **4**,
728 (10.12688/wellcomeopenres.15191.2)
- 729

730 Figure Legends

731 Figure 1. Model of the Ds/Ft system

732 (a, b) The anterior, or A compartment of a segment in the abdomen is shown. In
733 response to gradient(s) of morphogen(s), opposing supracellular gradients of Fj
734 and Ds are established. Fj predominates in the anterior region and Ds in the
735 posterior region. Fj affects the binding of Ds with Ft and consequently both the Fj
736 gradient and the gradient of Ds itself determine the distribution of Ds-Ft and Ft-
737 Ds in the cells. A cell determines its polarity by comparing the disposition of Ft
738 and/or Ds between its anterior and posterior membrane [10].

739 (c) How we isolate anterior or posterior membranes to measure tagged Ds in
740 each. All the cells contain normal amounts of Ds, half of which is tagged. Tagged
741 Ds is removed in small clones and replaced with normal untagged Ds.
742 Consequently, the tagged Ds in either only the posterior membrane (orange) or
743 only the anterior membrane (blue) of a cell flanking the clone can be measured.

744 Figure 2. The supracellular gradient and cellular asymmetry of Ds in wildtype 745 pupal epidermis

746 (a) All the measurements of Ds (both anterior and posterior cell membranes) are
747 plotted across an entire metamere (0-100% of compartment length). A and P
748 compartments are shown separately. The position of the compartment boundary
749 was determined by mapping the expression of *engrailed*. Supracellular gradients
750 are estimated to rise from the front to the back by 30% in the A compartment,
751 falling in the P compartment by 15%. The shaded area represents the 95%
752 confidence interval for the fitted curve.

753 (b) The data points from above separated into anterior (blue) and posterior
754 membranes (orange). Note both sets of data are graded but differ consistently in
755 relative Ds amounts (but see figures S1, S2). In the A compartment the amount of
756 Ds is greatest in the anterior membranes (peaking at about 40% near the middle
757 of the compartment). In the P compartment the amount Ds is greatest in the
758 posterior membranes.

759 **Figure 3. The supracellular gradient and cellular asymmetry of Ds in *ffj*- pupal**
760 **epidermis**

761 (a) and (b) compare with data shown in Figure 2, the gradients are similar but
762 somewhat shallower. In (a) note the loss of cellular asymmetry in the anterior
763 region of the A compartment.

764 (c) The wildtype and *ffj*- cell asymmetry data are both shown on one plot. The
765 anterior membranes, in both A and P compartments, have similar values in both
766 wildtype and *ffj*-. Note that, in the A compartment of *ffj*- pupae, there is less Ds on
767 the posterior membranes than in the wildtype, reducing the cellular asymmetry
768 everywhere but especially in the anterior region.

769 **Figure 4. Estimating the robustness of the Ds/Ft system in the A compartment.**

770 Clones overexpressing *fz* reverse polarity anterior to the clone and they do so by
771 overcoming the Ds/Ft system. In wildtype pupae the extent of reversal is more or
772 less uniform within the A compartment. However, in the absence of Fj, the Ds/Ft
773 system is weakened in the anterior regions as shown by increased range of
774 reversal, when compared to wildtype (The shaded area represents the 95%
775 confidence interval for the fitted curve).

776 **Figure 5. Asymmetric localisation of Dachs vis-à-vis A/P boundary**

777 Much of the areas shown is covered with clones lacking tagged D. We see from
778 islands of cells containing tagged D that D is located anterior in most cells of the
779 A compartment (a) and located posterior in cells of the P compartment (b). Note
780 that just within the A compartment, both near the anterior (c) and posterior
781 limits (d), 1 or 2 rows of cells evince a polarity characteristic of P cells, with D
782 located mainly on the posterior edges of the cells. The A/P boundary is
783 demarcated by the anterior edge of *engrailed* expression that marks all cells of
784 the P compartment (purple territory). Evidential membranes are marked with
785 arrowheads, blue for anterior membranes and beige for posterior.

786 **Figure 6 Clones overexpressing *ft* near the A/P compartment border**

787 (a) clone of A compartment provenance, reverses territory both in front (in A
788 territory) and behind (in P territory).

789 (b) clone of P compartment provenance, reverses the polarity of cells behind (in
790 P territory) but fails to reverse in front (A territory). White arrows show
791 estimated position of A/P borders, red dots mark clone boundaries.

792 (c) simplified diagram of above results; note line of polarity reversal shown by
793 the location of D is anterior to the A/P boundary by 1-2 cells (shaded zone) and
794 this explains the outcomes, see text; these results mimic those with *fj*-
795 overexpressing clones [20].

796 [Figure 7 Speculative model of the action of Fj on positioning of Ds-Ft](#)
797 [heterodimers. Why does the loss of Fj particularly affect the posterior](#)
798 [membranes of cells?](#)

799 Two places in the A compartment are shown

800 (a) 10% back from the anterior limit of the A compartment. In this area Fj is
801 largely responsible for the supracellular gradient and cellular asymmetry.
802 Phosphorylating Ds reduces its tendency to bind to Ft while phosphorylating Ft
803 increases its tendency to bind to Ds [17, 18]. The Ds phosphorylated by Fj is
804 shown to be inserted preferentially into the posterior membrane where it binds
805 to Ft in the abutting cell. We don't know why this might be so, it is possible that
806 phosphorylated Ds might be transported posteriorly in the cell.

807 Below, the same location but in *fj*⁻ pupae. There is no variation in cellular
808 asymmetry with position and the gradient is almost flat due to low levels of
809 available Ds in this area where there is now no Fj to drive polarity.

810 (b) 50% back from the anterior limit of the A compartment. In this area the
811 gradient of Ds is sufficient to drive both the supracellular gradient and the
812 cellular asymmetry, thus, below, in the absence of Fj, both the gradient and the
813 asymmetry persist with only some reduction in strength. As with (a) we imagine
814 phosphorylated Ds being added preferentially to the posterior membranes of
815 cells.

816

817 Supplementary Figures

818 **Figure S1** Bootstrapped estimates of the correlation between Ds accumulation at
819 cell membranes and their position within the segment, in wildtype and ff^-
820 abdomens.

821 Raincloud plots [58] of bootstrap estimates of correlation coefficients of the data
822 showed in **figures 2a** and **3a**. The estimates are clearly departing from zero in
823 both A compartments; most of the estimates of the estimates obtained for the
824 wildtype P compartment are negative, however, the correlation in ff^-
825 compartments appear to be lost.

826 **Figure S2** Estimated differences of trends in Ds accumulation

827 Differences of trends in Ds accumulation of pairs of smooths in anterior and
828 posterior cell membranes of the A compartments (a), and anterior and posterior
829 cell membranes of the P compartments (b) of wild type and ff^- .

830 **Figure S3** The location of D in ff^- pupae

831 (a) Images shows an anterior region of A compartment; in the wildtype all cells
832 of this region show D localised anteriorly. But in ff^- cells show either posterior
833 localisation of D (the anteriormost cells in the image) or variable or unclear
834 asymmetry.

835 (b) An area near the middle of the A compartment showing that D, as in wildtype
836 cells in this region, is located anteriorly.

837 Blue arrow marks an anterior membrane, with no D visible and orange arrow
838 marks the posterior membrane of a cell with some D posteriorly.

839 **Figure S4** To illustrate effects of ft overexpressing clones on bridges and
840 polarity

841 Upper row shows wildtype. Normally, in the A compartment most Ds is on the
842 anterior membrane (see **figure 2**) but the rearmost cell of the A compartment
843 has reversed Ds/Ft polarity (as shown by the localisation of D, see **figure 5**), with
844 most Ds on its posterior membrane. In the P compartment there is more Ds on
845 the posterior membrane

846 Middle row shows a clone overexpressing ft at the rear of the A compartment.
847 Cells of this clone (one cell is shown) draw Ds to the adjacent membranes on
848 both neighbours and both these neighbours polarities are reversed (cells
849 labelled in pink).

850 Bottom row shows a clone overexpressing ft at the front of the P compartment.
851 Cells of this clone draw Ds to the adjacent membranes on both neighbours but
852 only its neighbour in the P compartment has its polarity reversed (cells labelled
853 in pink). The neighbour in the A compartment retains its normal normal polarity
854 (see Figure 6).

855

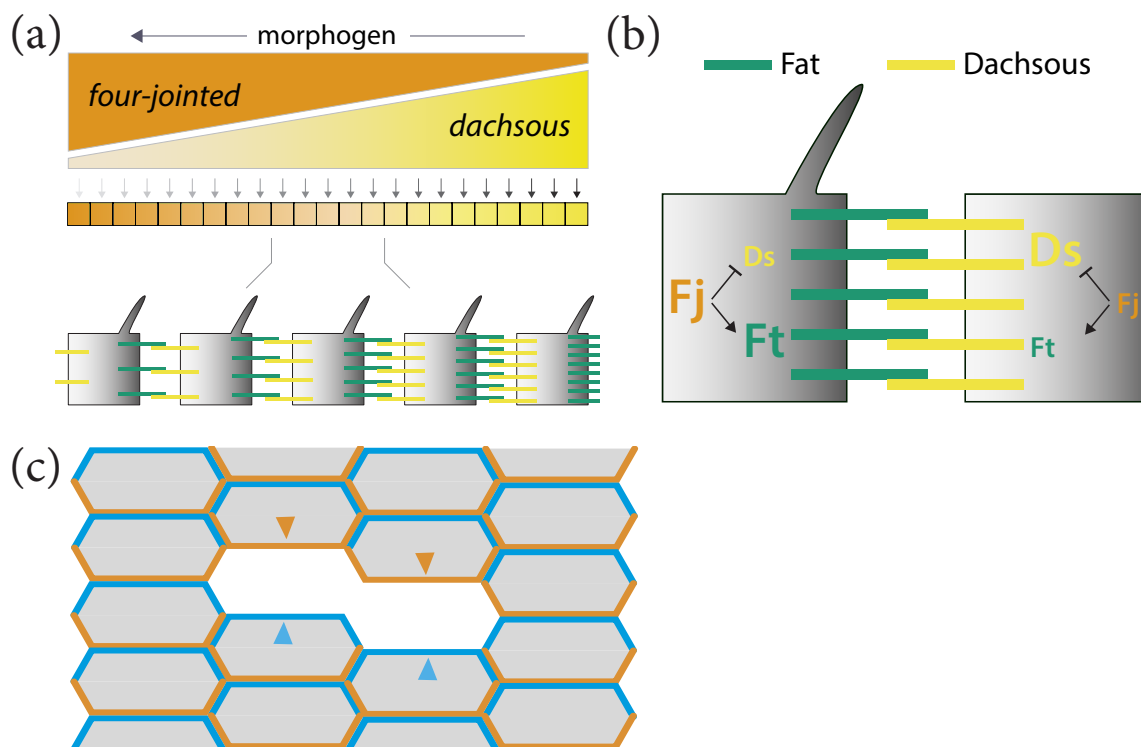
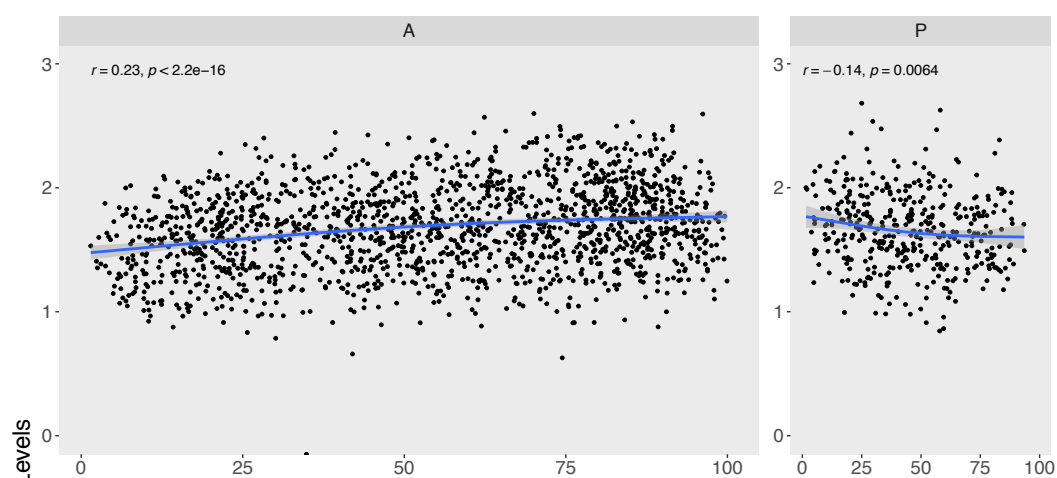


Figure 1

Ds gradient in the pupal abdomen *wildtype*

(a)



(b)

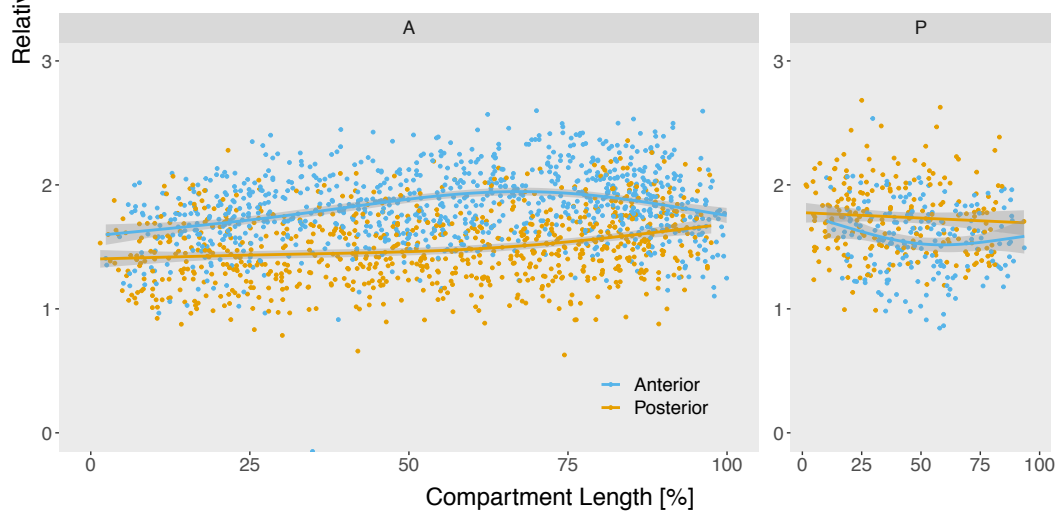
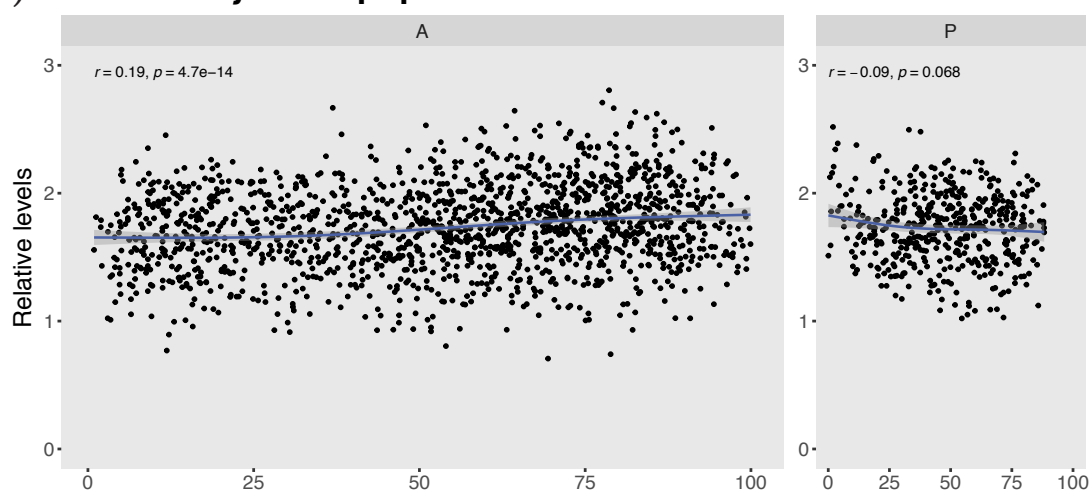
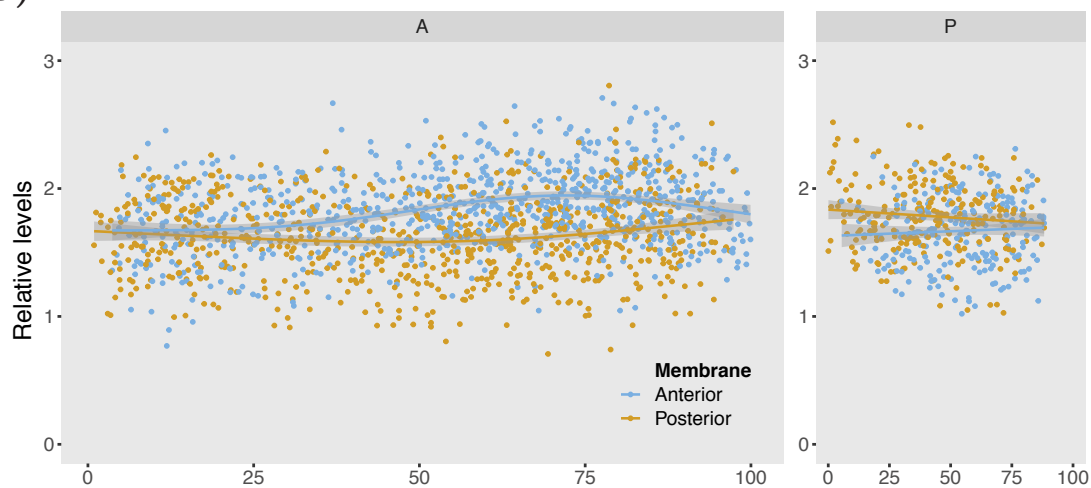


Figure 2

(a) **Ds in *four-jointed* pupal AEC**



(b)



(c) **Ds in *wild type* & *four-jointed* pupal AEC**

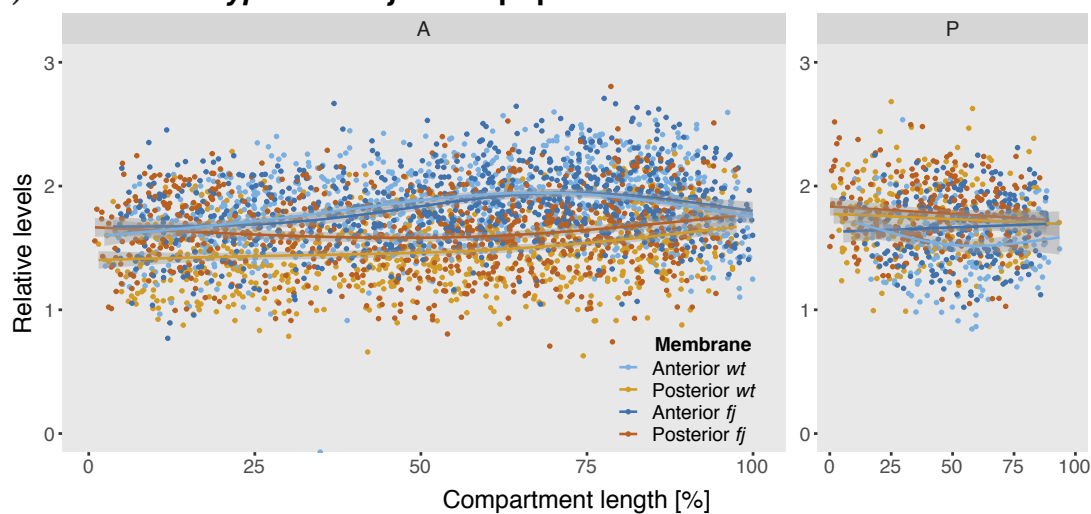


Figure 3

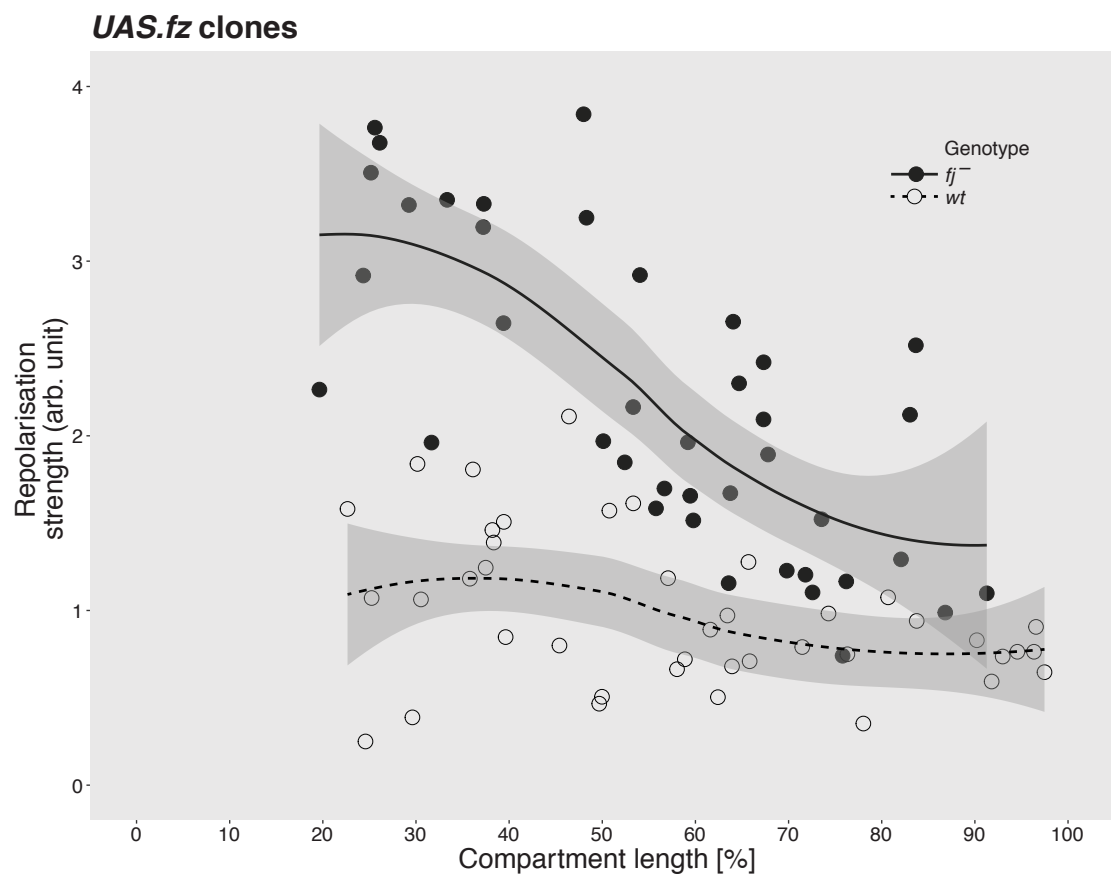


Figure 4

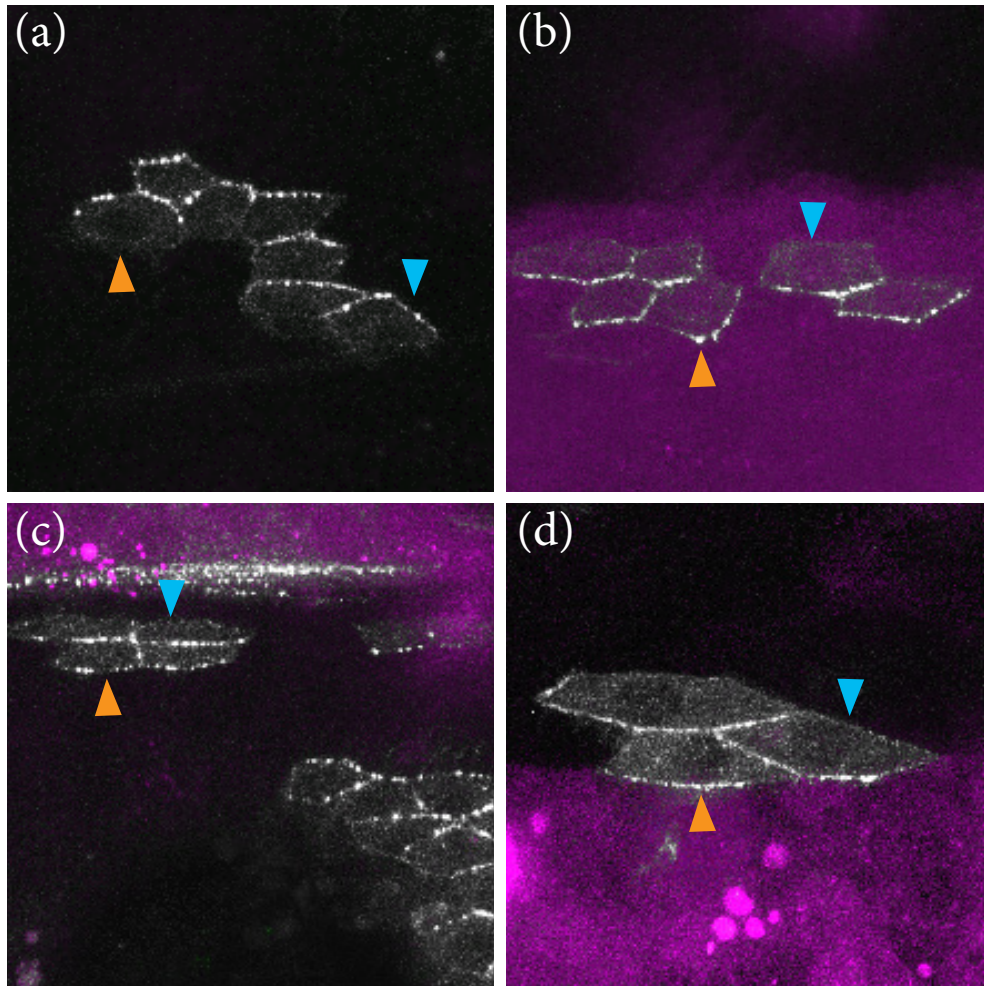


Figure 5

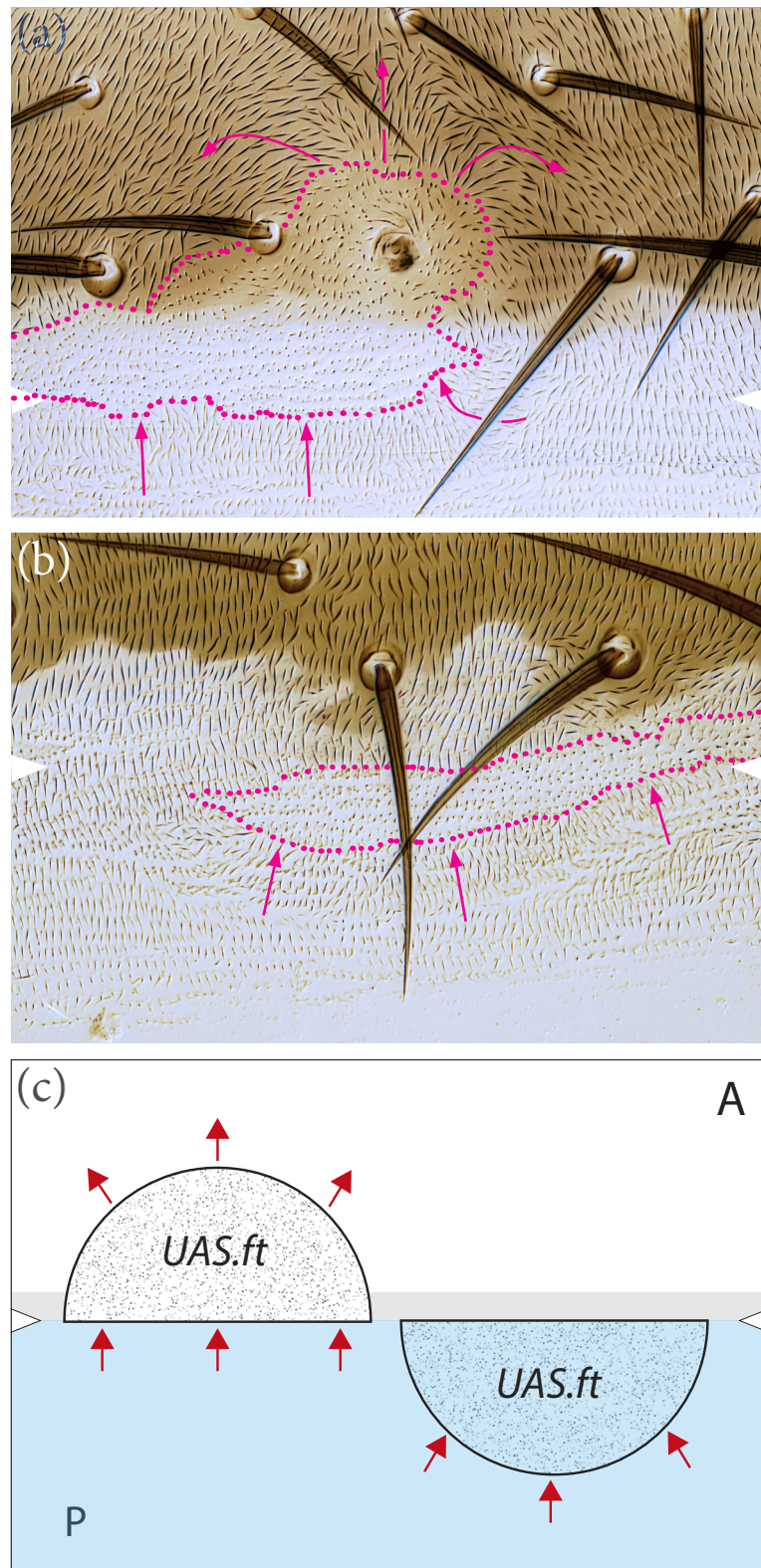
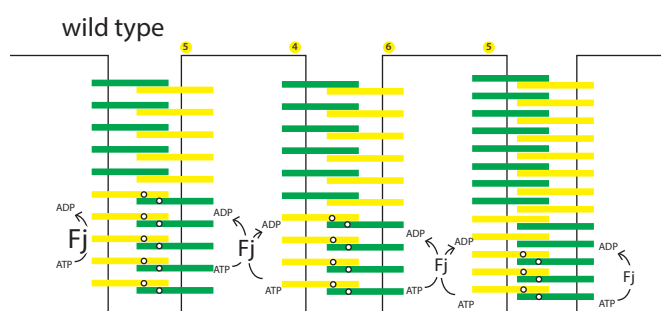
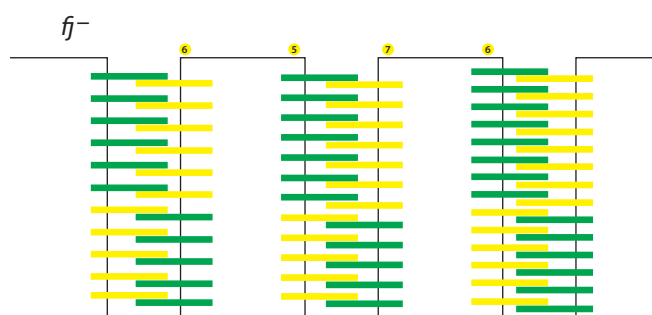
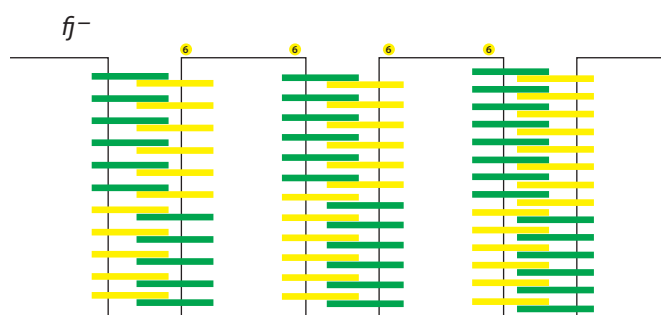
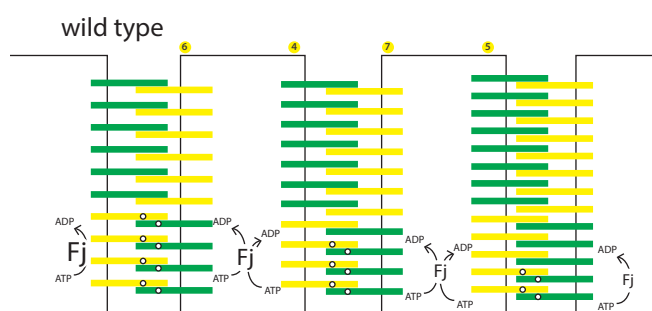


Figure 6

snapshot at 10% of the A compartment



snapshot at 50% of the A compartment



— Ds — Ft ○ PO₄

Figure 7

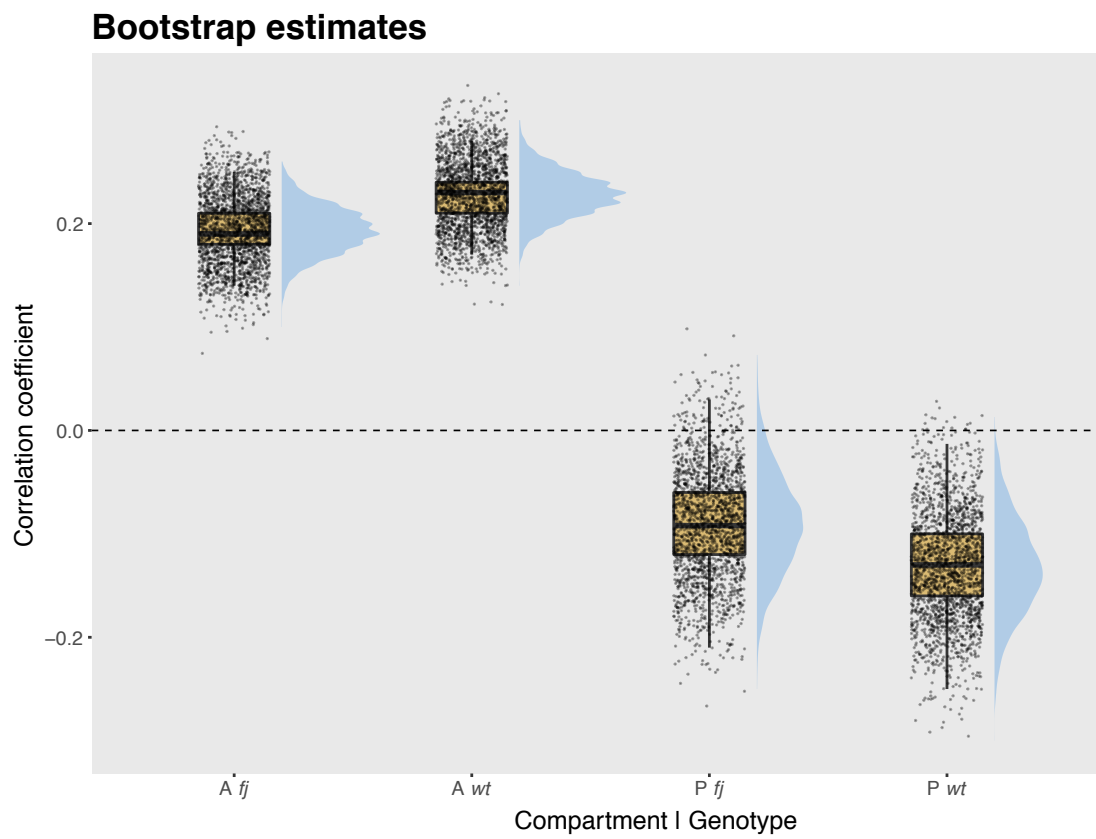


Figure S1

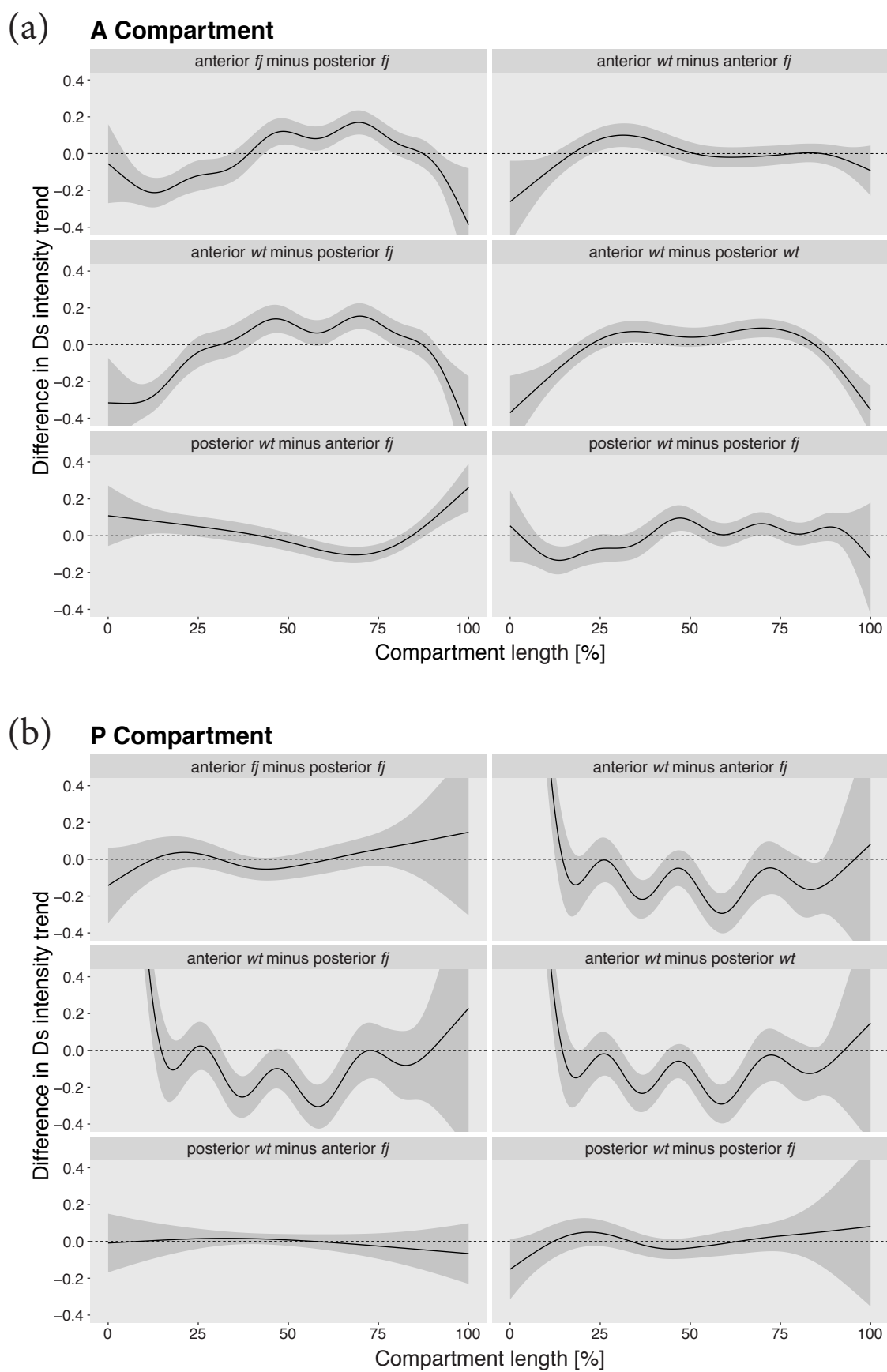


Figure S2

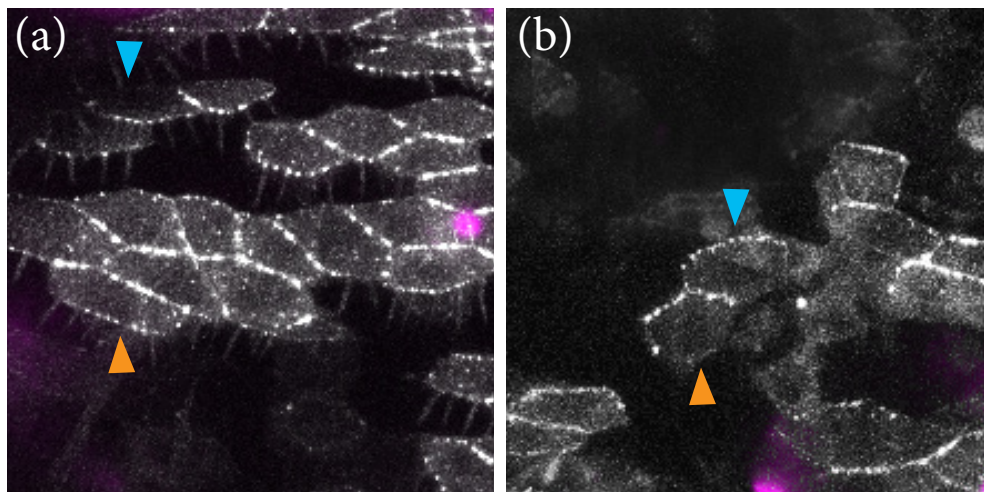


Figure S3

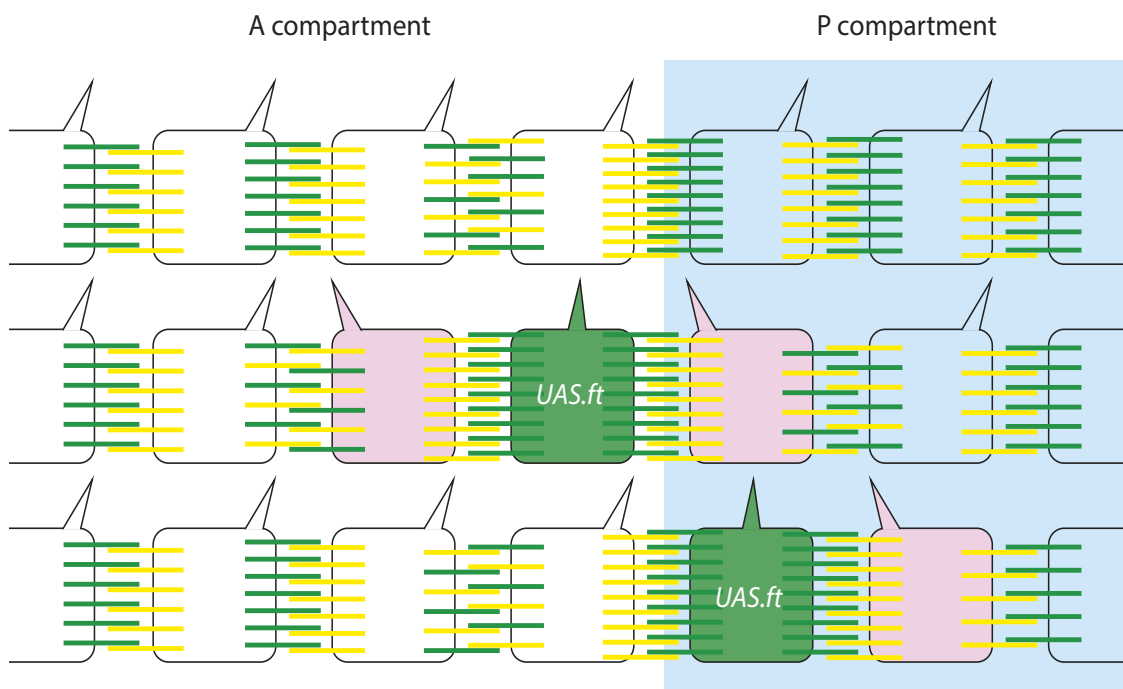


Figure S4